Y_2BaNiO_5: A nearly ideal realization of the $S=1$ Heisenberg chain with antiferromagnetic interactions

Guangyong Xu
Department of Physics and Astronomy, The Johns Hopkins University, Baltimore, Maryland 21218

J. F. DiTusa
Department of Physics and Astronomy, Louisiana State University, Baton Rouge, Louisiana 70803

T. Ito and K. Oka
Electrotechnical Laboratory, Tsukuba 305, Japan

H. Takagi
The Institute for Solid State Physics, University of Tokyo, Roppongi, Tokyo 106, Japan

C. Broholm
Department of Physics and Astronomy, The Johns Hopkins University, Baltimore, Maryland 21218 and National Institute of Standards and Technology, Gaithersburg, Maryland 20899

G. Aeppli
NEC Research Institute, 4 Independence Way, Princeton, New Jersey 08540

(Received 4 June 1996)

We report an inelastic-neutron-scattering experiment on single crystals of the one-dimensional spin-one antiferromagnet Y_2BaNiO_5. The data show that this compound is a nearly ideal material for studying the Haldane conjecture in the Heisenberg limit. In particular, the Haldane gap at $\tilde{q}=\pi$ is almost isotropic, taking on the values of 7.5(1), 8.6(1), and 9.6(1) meV for polarizations parallel to the three principal orthorhombic axes respectively. Interchain coupling along the edges of the orthorhombic unit cell is found to be very weak ($J'/J \leqslant 5\times 10^{-4}$). Finally, we show that defects in our sample at the 1% level cause visible broadening of the excitation at $\tilde{q}=\pi$. [S0163-1829(96)52034-5]

In 1983 Haldane showed that antiferromagnetic integer spin chains have a singlet ground state separated from a band of triplet excited states by a finite energy gap.[1] Since then a plethora of theoretical,[2–4] numerical,[5–8] and experimental[9–14] work has confirmed these results and provided additional insight into this unique magnetic phase. Experimental progress in the field is controlled by the discovery of suitable quasi-one-dimensional model systems. The systems studied until now were primarily organic dielectrics, however, recently a family of transition metal oxides, R_2BaNiO_5, which also display the Haldane gap was discovered.[15] These materials are leading the research in new directions. For example, partial substitution of divalent cations such as Ca^{2+} on the normally trivalent rare-earth (R^{3+}) site places mobile holes on the NiO_5 spin chains with interesting charge and spin dynamics.[16,17] Another fascinating aspect is the antiferromagnetic order which occurs when the R^{3+} ion is magnetic.[18] To understand these magnetic phenomena, it is important to know the spin Hamiltonian for Ni^{2+} ions in R_2BaNiO_5. This information is best obtained through studies of the simplest member of the family : Y_2BaNiO_5. Previous neutron-scattering experiments on powder samples and small single crystals of Y_2BaNiO_5 showed a Haldane gap of approximately 9 meV.[19–21] Here we report a neutron-scattering study of a large Y_2BaNiO_5 single crystal which determines the spin-space anisotropy and interchain coupling in this material.[22]

Y_2BaNiO_5 has a body-centered orthorhombic structure, space group *Immm* (Ref. 23) with lattice parameters $a=3.7648$ Å, $b=5.7550$ Å, and $c=11.324$ Å at $T=10$ K. We index momentum transfer in the corresponding reciprocal lattice $\mathbf{Q}=h\mathbf{a}^*+k\mathbf{b}^*+l\mathbf{c}^*$. The material contains isolated chains of corner sharing NiO_6 octahedra. Ni atoms within a chain are separated by $\mathbf{a}$ so we use $\tilde{q}=\mathbf{Q}\cdot\mathbf{a}=2\pi h$ to denote wave vector transfer along the spin chain.

Unpolarized magnetic neutron scattering measures the convolution of a well-defined resolution function[24] with the following linear combination of Cartesian components of the dynamic spin correlation function:[25]

$$I(\mathbf{Q},\omega)=\sin^2\theta S^{aa}(\mathbf{Q},\omega)+(1-\sin^2\theta\cos^2\phi)S^{bb}(\mathbf{Q},\omega)+(1-\sin^2\theta\sin^2\phi)S^{cc}(\mathbf{Q},\omega). \quad (1)$$

Here (θ,ϕ) are polar angles for wave vector transfer, $\mathbf{Q}$, $(\hat{\mathbf{Q}}\cdot\hat{\mathbf{a}}=\cos\theta)$. In this experiment we report data for $\mathbf{Q}$ in the $(hk0)$ and $(h0l)$ planes of the reciprocal lattice corresponding to $\phi=0$ and $\phi=\pi/2$ respectively. Normalization of magnetic-scattering intensities to the integrated intensity of acoustic phonons and assuming that $g=2$ allow us to report data in units of 1/meV defined such that $\int d^3\mathbf{Q}\int\hbar\,d\omega\,\Sigma_\alpha S^{\alpha\alpha}(\mathbf{Q},\omega)/\int d^3\mathbf{Q}=S(S+1)$, where $S=1$ is the spin quantum number for the Ni ions.

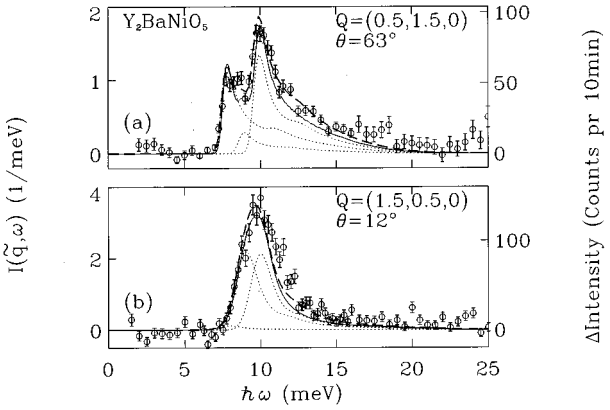

FIG. 1. Background subtracted constant-**Q** scans. Collimations were 40′-40′-40′-80′ and $E_f=14.7$ meV on BT4. At $\hbar\omega=10$ meV, the FWHM energy resolution is $\Delta E=1.6$ meV while the wave-vector resolutions along the chain are $\Delta\tilde{q}/\pi = 0.110$ and 0.048 for frames (a) and (b) respectively. Solid lines are from the global fit. Dashed lines include the effects of a chain severing defect density of 1%. Dotted lines show contributions from each mode of polarization.

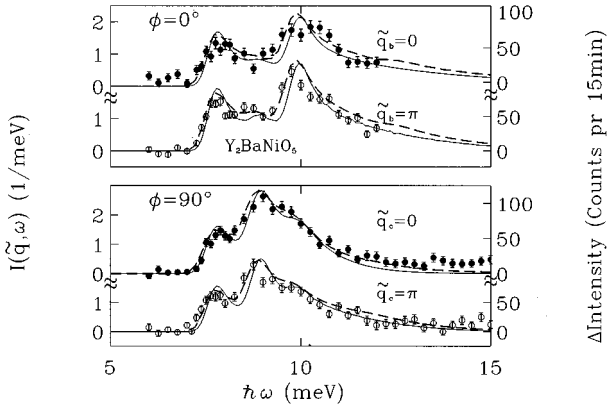

FIG. 2. Background subtracted constant-**Q** scans in the $(hk0)$ (top frame), and $(h0l)$ (bottom frame) zones where $\phi=0$ and $\pi/2$ respectively [see Eq. (1)]. Wave-vector transfer from top to bottom was (0.5,2,0), (0.5,1.5,0), (0.5,0,2) and (0.5,0,2.5). Collimations were 20′-20′-40′-100′, and $E_f=13.7$ meV on BT2. At $\hbar\omega=10$ meV, the energy resolution was 1.07 meV (FWHM) and the wave vector resolutions along the chain are $\Delta\tilde{q}/\pi = 0.08$, 0.104, 0.060, and 0.040, respectively (from top to bottom). Solid and dashed lines are described in the caption to Fig. 1.

Our sample consists of two single crystals of Y_2BaNiO_5 with total mass 0.72 g which were kept at $T=10$ K in a displex. The experiments were performed on the pyrolytic graphite (PG) based thermal neutron triple axis spectrometers BT2 and BT4 at NIST. We used the fixed final energy mode with $E_f=13.7$ meV and $E_f=14.7$ meV and a 2.5-cm-thick PG filter before the analyzer. Apart from magnetic scattering, nuclear incoherent scattering and fast neutrons also contribute to the detector count rate. These background contributions varied from two to four counts per min. with Q and $\hbar\omega$ but, unlike the magnetic scattering, do not depend significantly on sample orientation ($\hat{\mathbf{Q}}$). Thus for each constant-**Q** scan we subtracted the $\hat{\mathbf{Q}}$-independent background determined from similar scans with the sample rotated sufficiently to eliminate magnetic scattering in the range of energies probed.

Figure 1 shows two spectra for symmetry-related values of **Q** corresponding to $\tilde{q}=\pi$. Magnetic neutron scattering at the magnetic zone center occurs only at finite $\hbar\omega$ which is evidence for the Haldane gap in this material. Both scans were performed for **Q** in the $(hk0)$ zone ($\phi=0$), but the angle, θ, between **Q** and the chain axis is different for the two scans. The strongest peak in both scans is at $\hbar\omega\approx$ 9.8 meV. In Fig. 1(a) where $\theta=63°$, a second peak appears at $\hbar\omega\approx7.6$ meV. The fact that this peak is not visible in Fig. 1(b) where **Q** is almost parallel to the chain axis ($\theta=12°$) proves that the 7.6 meV mode is associated with magnetic fluctuations polarized along the chain axis [Eq. (1)]. A previous neutron-scattering experiment on a powder sample[19] showed an additional peak for $\hbar\omega=16$ meV. Our data show that there is no peak in the magnetic scattering for $\hbar\omega=16$ meV and $\tilde{q}=\pi$. The peak observed in the powder experiment could either be nonmagnetic or could result from magnetic scattering at a different value of **Q**.

The data in Fig. 1 also indicate that the two transverse modes are not degenerate. In Fig. 1(a) there is more intensity between 7.6 and 9.8 meV than can be accounted for by two resolution limited modes. Moreover the peak in Fig. 1(b), which comes almost exclusively from transverse spin fluctuations, is much broader than our resolution. Additional evidence for the splitting of the transverse modes is provided by Fig. 2, where we compare higher resolution constant $\tilde{q}=\pi$ scans for $\phi=0$ [$(hk0)$ zone] and $\phi=\pi/2$ [$(h0l)$ zone]. According to Eq. (1) spin fluctuations perpendicular to the scattering plane always contribute to $I(\mathbf{Q},\omega)$. Indeed, other things being equal, S^{cc} accounts for half of the spectral weight for any **Q** in the $(hk0)$ plane. A mixture of S^{aa} and S^{bb} accounts for the other half, implying that if **Q** is neither along $\hat{\mathbf{a}}$ nor $\hat{\mathbf{b}}$, and if S^{aa}, S^{bb}, and S^{cc} are peaked at resolvably different energies, S^{cc} will yield the most pronounced feature in $I(\mathbf{Q},\omega)$. Similarly, S^{bb} will dominate $I(\mathbf{Q},\omega)$ in the $(h0l)$ plane. Clearly the strongest peak in $I(\mathbf{Q},\omega)$ occurs at higher energy for $(hk0)$ zone data than for $(h0l)$ zone data. Interchain coupling cannot account for this energy shift since no corresponding shift is seen in the lowest-energy longitudinal mode. Furthermore, the data labeled $\tilde{q}_b=0$ and $\tilde{q}_c=0$ in Fig. 2 were collected at symmetry related values of **Q**. We conclude that anisotropy transverse to the spin chain creates separate gaps at 8.8 and 9.8 meV for spin fluctuations along the **b** and **c** directions respectively.

Having determined the gap energies using constant-**Q** scans, we performed constant-$\hbar\omega$ scans at higher energies to determine the velocity of spin excitations along the chain. The data are shown in Fig. 3. The peaks were fitted to Gaussians whose positions are summarized in Fig. 4. To extract accurate values of gaps and spin wave velocities and to determine whether the peaks are resolution limited, we compare the data to a model for the dynamic spin correlation function which is based on the ''single mode approximation''[26,27]

$$S^{\alpha\alpha}(\tilde{q},\omega)=\frac{2}{3}(-\langle\mathcal{H}\rangle/L)\frac{1-\cos\tilde{q}}{\hbar\omega_\alpha(\tilde{q})}\delta[\hbar\omega-\hbar\omega_\alpha(\tilde{q})]. \quad (2)$$

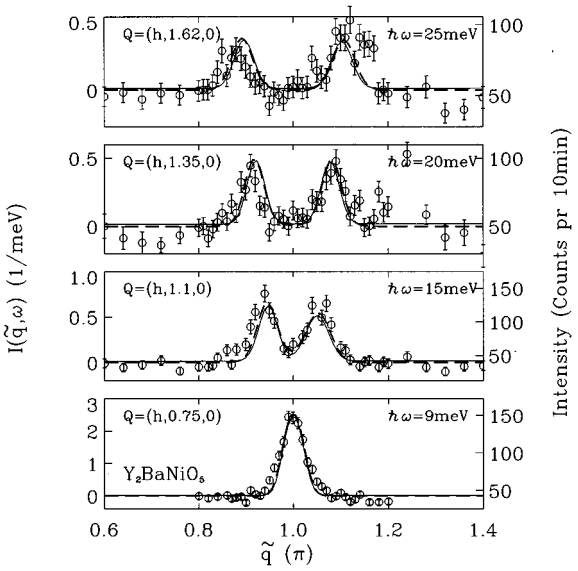

FIG. 3. Constant energy transfer scans with collimations 60′-20′-40′-100′, 60′-20′-40′-100′, 40′-40′-40′-80′ and 20′-20′-40′-100′; fixed final energies E_f of 13.7, 13.7, 14.7, and 13.7 meV; energy resolutions (ΔE) of 2.75, 2.31, 2.10, and 1.04 meV; and wave-vector resolutions ($\Delta\tilde{q}/\pi$) along the chain of 0.04, 0.04, 0.04, and 0.034, respectively (from top to bottom). Solid and dashed lines are described in the caption to Fig. 1.

For $\hbar\omega_\alpha(\tilde{q})$ we use the following form which was found to account for data in $Ni(C_2H_8N_2)_2NO_2ClO_4$ (NENP):[12]

$$\hbar\omega_\alpha(\tilde{q}) = \sqrt{\Delta_\alpha^2 + v^2\sin^2\tilde{q} + A\cos^2\frac{\tilde{q}}{2}}. \tag{3}$$

The solid lines in Figs. 1–3 are the result of a global fit of Eqs. (1)–(3) to all our data. The energies of the three gaps, the spin wave velocity, the ground-state energy ($\langle\mathcal{H}\rangle/L$) and flat backgrounds for constant energy transfer scans were varied. Our data for $\tilde{q}\approx\pi$ is insensitive to the value of A so this parameter was fixed to 170 meV[2]. The value obtained by scaling A for NENP by the squared ratio of the mode averaged energy gap for the two materials. The reasonable overall agreement between the model (solid lines in Figs. 1–3) and data ($\chi^2=3.8$) indicates that the single mode approximation provides an acceptable description of dynamic spin correlations in Y_2BaNiO_5. The energies of the three modes obtained in this global fit are $\Delta_a=$ 7.7(1) meV, $\Delta_b=8.8(1)$ meV, and $\Delta_c=9.8(1)$ meV. Note, however, that peaks in the data in general appear broader than predicted by the model [see, e.g., Fig. 1(a) for $\hbar\omega\approx8$ meV]. This is surprising since experiments on other $S=1$ spin chains[12] and numerical simulation[6] indicate that the Haldane mode for $\tilde{q}\approx\pi$ and $k_BT\ll\Delta$ is long lived. Likely causes for the broadened peaks are chain severing defects in our sample.[16,20] For an isolated chain with L Ni^{2+} spins, the energy of the lowest-lying one-magnon state is approximately Ref. 7 $\Delta(L)=\sqrt{\Delta^2(\infty)+v^2\sin^2[\pi(1-1/L)]}$, where $\Delta(\infty)$ is the value of the gap for the infinite length chain. In a sample with a chain-severing defect concentration, c, there exists a Poisson distribution, $P(L)=Lc^2(1-c)^L$ of chains with different lengths, L, and hence a distribution of energy gaps. In addition there is quantization of $\tilde{q}$ (in steps of $1/L$) for finite length chains. Given imperfect spectroscopic resolution, these effects broaden the peaks in $S(\tilde{q},\omega)$. To determine their relevance to our experiment, we measured the magnetic susceptibility of a small fragment of our sample. Apart from the exponentially activated susceptibility associated with the Haldane gap, we found a Curie tail with a strength corresponding to 1.9(2) % spin-1/2 impurities per Ni^{2+} ion. Assuming that a chain severing defect adds two spin-1/2 degrees of freedom,[28–31] the concentration of such defects is $c=1.0(1)$ %. We then modeled $S(\tilde{q},\omega)$ in a single finite-length spin chain by displacing the dispersion relation to the energy of the lowest-lying one-magnon mode, $\Delta(L)$, and convoluting with a Gaussian in $\tilde{q}$ with full width at half maximum (FWHM) $1/L$. To account for the random location of defects along the spin chains we summed dynamic correlation functions for the ten representative chain lengths weighted according to the Poisson distribution. Fitting to this model, which had no more adjustable parameters than the previous fit, yielded a significantly better fit to the data ($\chi^2=2.8$) as is apparent from the dashed lines in Figs. 1–3. Thus chain severing defects *could be* the reason for the broadening of peaks in constant-$\tilde{q}$ scans observed in our sample.[20] The infinite chain length gap values derived from this fit were $\Delta_a=7.5(1)$ meV, $\Delta_b=8.6(1)$ meV, and $\Delta_c=9.6(1)$ meV. The average gap energy is $\bar{\Delta}=(\Delta_a+\Delta_b+\Delta_c)/3=8.6(1)$ meV.

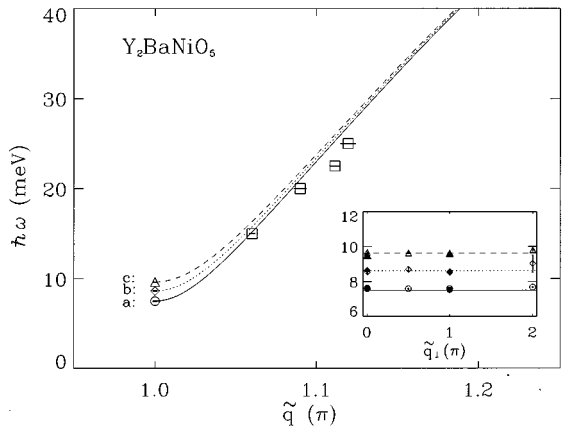

FIG. 4. Dispersion relation for magnetic excitations in Y_2BaNiO_5. The lines are our best estimate of the dispersion relation for infinite length spin chains obtained from a global fit to all data taking into account resolution effects and 1% chain severing defects in our sample. The points for $\tilde{q}=\pi$ were obtained through fits of the same model to single constant $\tilde{q}$ scans. The points at higher energies were obtained by Gaussian fits to the data in Fig 3. The inset shows the dependence of the $\tilde{q}=\pi$ energy gaps on wave-vector transfer $\tilde{q}_{\perp b}=2\pi k$ (open symbols) and $\tilde{q}_{\perp c}=2\pi l$ (filled symbols).

We now discuss the implications of our experiment for the magnetic Hamiltonian of Y_2BaNiO_5. The key result is the nearly isotropic nature of the Haldane gap in Y_2BaNiO_5, which implies that to a very good approximation an appropriate starting point is that for an antiferromagnetic Heisenberg chain with exchange parameter $J\approx\bar{\Delta}/0.4105=21$ meV.[7] This value is about 20% lower than the value $|J|\approx285K=24.6$ meV deduced from susceptibility

measurements.[19] The spin wave velocity $v=70(5)$ meV, which when divided by Δ yields a correlation length $\xi=v\Delta=8.1(6)$. This value is slightly larger than for the Heisenberg $S=1$ chain where $\xi=6.03$.[7] Finally from the prefactor to the fit we obtain $\langle \mathcal{H}/LJ\rangle=-1.3(2)$ which is close to the value $-1.4015(5)$ (Ref. 5) obtained from numerical calculations.

From our data, we cannot distinguish between single-ion anisotropy and exchange anisotropy. If we assume, as is customary in the field, that exchange anisotropy can be neglected, the relevant anisotropy terms in the spin Hamiltonian are $DS_z^2+E(S_x^2-S_y^2)$ where x,y, and z denote the c,b, and a axis, respectively. Numerical calculations[8] for the uniaxial $S=1$ chain ($E=0$) show that $\Delta_\perp=\Delta_0-0.57D$ and $\Delta_\parallel=\Delta_0+1.41D$, where Δ_0 is the gap value in the absence of anisotropy. If we take $\Delta_\perp$ to be the average of the transverse mode energies in Y_2BaNiO_5, we obtain $\Delta_0\approx 8.6$ meV and $D\approx -0.81$ meV (easy-axis anisotropy). For $D/J=0.18$ the splitting of the transverse modes equals $4E$.[8] Using this result to estimate a value for E in Y_2BaNiO_5 yields $E\approx 0.25$ meV.

To determine the strength of interchain coupling along the b and c directions, we performed constant $\tilde{q}=\pi$ scans varying the wave-vector components perpendicular to the chain. No dispersion is visible in our data (Fig. 2 and inset to Fig. 4) and this allows us to place an upper limit of 0.25 meV on any dispersion along these directions for $\tilde{q}=\pi$. An upper bound on the interchain couplings $J'_{b,c}$ is obtained using the classical spin-wave expression for the dispersion of the $\tilde{q}=\pi$ gap in a body-centered orthorhombic easy axis antiferromagnet.[25] We find $|J'_{b,c}|\leqslant[(\Delta_0+0.25)^2-(\Delta_0)^2]/(16S^2\,J)\sim 0.012$ meV so the ratio $|J'_{b,c}/J|\leqslant 5\times10^{-4}$. This is more than one order of magnitude smaller than the critical ratio $|J'/J|\approx 0.4/z'(\Delta_0/J)^2\approx 1.3\times10^{-2}$ required to induce a magnetically ordered ground state.[32,33] Here $z'=4$ is the chain coordination number corresponding to $J_{b,c}$. Note, however, that our data are insensitive to exchange coupling between the corner and body-centered Ni^{2+} ions because the effects of this frustrated interaction tend to cancel for $\tilde{q}\approx\pi$. Comparing different materials we have $D/J=-3.9\times10^{-2}$ and $|J'/J|<5\times10^{-4}$ for Y_2BaNiO_5 whereas $D/J=-1.9\times10^{-2}$ and $|J'/J|=2\times10^{-2}$ for $CsNiCl_3$ (Ref. 9), $D/J=0.18$ and $|J'/J|=8\times10^{-4}$ for NENP (Ref. 13) and $D/J=5.8\times10^{-3}$ (Ref. 34) and $|J'/J|\approx10^{-5}$ for $AgVP_2S_6$.[14]

In summary, spin space anisotropy and interchain couplings are relatively weak perturbations in Y_2BaNiO_5. They lead to splitting of the Haldane gap for $\tilde{q}=\pi$ into three modes at $\Delta_a=7.5(1)$ meV, $\Delta_b=8.6(1)$ meV, and $\Delta_c=9.6(1)$ meV with less than 0.25 meV dispersion for wave-vector transfer perpendicular to the spin chains. The magnetic phenomena which occur in derivatives of this material thus take place in a system whose underlying Hamiltonian is that of a nearly perfect Heisenberg chain with antiferromagnetic interactions between neighboring $S=1$ ions.

J.F.D. acknowledges the support of the Louisiana Board of Regents through the Louisiana Education Quality Support fund under Contract No. LEQSF(RF/1995-96)-RD-A-38. Work at JHU was supported by the NSF through Grant No. DMR-9302065 and Grant No. DMR-9453362.

[1] F. D. M. Haldane, Phys. Lett. A **93**, 464 (1983); Phys. Rev. Lett. **50**, 1153 (1983).
[2] I. Affleck *et al.*, Phys. Rev. Lett. **59**, 799 (1987).
[3] D. P. Arovas, A. Auerbach, and F. D. M. Haldane, Phys. Rev. Lett. **60**, 531 (1988).
[4] M. den Nijs and K. Rommelse, Phys. Rev. B **40**, 4709 (1989).
[5] M. P. Nightingale and H. Blöte, Phys. Rev. B **33**, 659 (1986).
[6] J. Deisz *et al.*, Phys. Rev. B **42**, 4869 (1990); S. V. Meshkov, *ibid.* **48**, 6167 (1993).
[7] S. R. White and D. A. Huse, Phys. Rev. B **48**, 3844 (1993).
[8] O. Golinelli, Th. Jolicoeur, and R. Lacaze, Phys. Rev. B **45**, 9798 (1992); **50**, 3037 (1994).
[9] R. M. Morra *et al.*, Phys. Rev. B **38**, 543 (1988).
[10] W. J. L. Buyers *et al.*, Phys. Rev. Lett. **56**, 371 (1986).
[11] J. P. Renard *et al.*, J. Appl. Phys. **63**, 3538 (1988).
[12] S. Ma *et al.*, Phys. Rev. Lett. **69**, 3571 (1992).
[13] L. P. Regnault *et al.*, Phys. Rev. B **50**, 9174 (1994).
[14] H. Mutka *et al.*, Phys. Rev. B **39**, 4820 (1989).
[15] St. Schiffler and X. Müller-Buschbaum, Z. Anorg. Allg. Chem. **532**, 10 (1986).
[16] J. F. DiTusa *et al.*, Phys. Rev. Lett. **73**, 1857 (1994).
[17] K. Kojima *et al.*, Phys. Rev. Lett. **74**, 3471 (1995).
[18] A. Zheludev *et al.* (unpublished).
[19] J. Darriet and L. P. Regnault, Solid State Commun. **86**, 409 (1993).
[20] J. F. DiTusa *et al.*, Physica B **194-196**, 181 (1994).
[21] T. Yokoo *et al.*, J. Phys. Soc. Jpn. **64**, 3651 (1996).
[22] We recently received a preprint from T. Sakaguchi *et al.* which arrives at conclusions similar to ours.
[23] E. Garcia-Matres *et al.*, J. Solid State Chem. **103**, 322 (1993); D. J. Buttrey *et al.*, *ibid.* **88**, 291 (1990).
[24] N. D. Chesser and J. D. Axe, Acta Crystallogr. Sect. A **29,** 160 (1973).
[25] S. W. Lovesey, *Theory of Neutron Scattering from Condensed Matter* (Clarendon, Oxford, 1984).
[26] R. P. Feynmann, *Statistical Mechanics* (Benjamin, Reading, MA, 1972).
[27] S. M. Girvin, A. H. MacDonald, and P. M. Platzman, J. Magn. Magn. Mater. **54-57**, 1428 (1985).
[28] T. Kennedy, J. Phys. Condens. Matter **2**, 5737 (1990).
[29] A. P. Ramirez *et al.*, Phys. Rev. Lett. **72**, 3108 (1994).
[30] S. H. Glarum *et al.*, Phys. Rev. Lett. **67**, 1614 (1991).
[31] P. P. Mitra *et al.*, Phys. Rev. B **45**, 5299 (1994).
[32] T. Sakai and M. Takahashi, Phys. Rev. B **42**, 1090 (1990); **42**, 4537 (1990).
[33] Y. A. Kosevich and A. V. Chubukov, Sov. Phys. JETP **64**, 654 (1986).
[34] M. Takigawa *et al.*, Phys. Rev. Lett. **76**, 2173 (1996); Phys. Rev. B **52**, R13 087 (1995).